

# Exact Solution to Finite Temperature SFDM: Natural Cores without Feedback

Victor H. Robles\* and T. Matos\*\*

*Departamento de Física, Centro de Investigación y de Estudios Avanzados del IPN, AP 14-740, 0700 D.F., México*

## ABSTRACT

Recent high-quality observations of low surface brightness (LSB) galaxies have shown that their dark matter (DM) halos prefer flat central density profiles. On the other hand the standard cold dark matter model simulations predict a more cuspy behavior. One mechanism to reconcile the simulations with the observed data is the feedback from star formation, this might be successful in isolated dwarf galaxies but its success in LSB galaxies remains unclear. Additionally, including too much feedback in the simulations is a double-edged sword, in order to obtain a cored DM distribution from an initially cuspy one, the feedback recipes usually require to remove a large quantity of baryons from the center of galaxies, unfortunately they also produce twice more satellite galaxies of a given luminosity than what is observed. Therefore, one DM profile that produces cores naturally and that does not require large amounts of feedback would be preferable. We find both requirements to be satisfied in the scalar field dark matter model. Here, we consider that the dark matter is an auto-interacting real scalar field in a thermal bath at temperature  $T$  with an initial  $Z_2$  symmetric potential, as the universe expands the temperature drops so that the  $Z_2$  symmetry is spontaneously broken and the field rolls down to a new minimum. We give an exact analytic solution to the Newtonian limit of this system and show both, that it satisfies the two desired requirements and that the rotation curve profile is not longer universal.

*Subject headings:* galaxies:formation–galaxies:halos —galaxies:individual (NGC 1003, NGC 1560, NGC 6946)–galaxies:fundamental parameters

## 1. Introduction

The longstanding core/cusp discussion, whether the central dark matter (DM) profiles in dwarfs and low surface brightness (LSB) galaxies are more core-like and rounder than the standard cold dark matter (CDM) model predicts, remains an open issue (van Eymeren et al. (2009); see de Blok (2010) for a recent review). So far, the core profiles most frequently used in the literature and that best fit the observations are empirical (Burkert 1995; Kuzio de Naray et al. 2010). Though they are useful to characterize properties of galaxies, it is necessary to find a theoretical framework which naturally produces

the cores, especially since more and more recent high-quality observations of LSB galaxies suggest that the core-like behavior ( $\rho \sim r^{-0.2}$ ) is preferred in the central regions of dwarf and LSB galaxies (Oh et al. 2011; Robles & Matos 2012; de Blok et al. 2001). This is a problem to the CDM model which prefers  $\rho \sim r^{-1}$  at small  $r$  (Navarro et al. 2010). Though the latest simulations can reach  $\rho \sim r^{-0.8}$  (Navarro et al. 2010; Merrit et al. 2006; Graham et al. 2006), which is not in total agreement with observations.

The current trend to solve the core/cups discrepancy in the CDM model is to include the dynamics of the baryonic component into DM simulations (Governato et al. 2010, 2012; Macio et al. 2011; Stinson et al. 2011; Romano-Daz et al. 2008). By including feedback from star formation in sim-

---

\*Electronic address: vrobles@fis.cinvestav.mx

\*\*Electronic address: tmatos@fis.cinvestav.mx

ulations of field dwarf galaxies, Governato et al. (2012) managed to change an initially cuspy DM halo into a core-like halo. On the other hand, Sawala et al. (2012) find in their simulations twice as many satellites of a given luminosity around a Milky Way size host halo. They found this by considering, in addition to feedback, the effect that surrounding galaxies have on its host halo by means of tidal interaction. This means, satellite galaxies are too luminous. They also find that the DM halos of satellites are more strongly affected than their stellar component by tidal interactions, and that, in the case that cores are a universal feature of dwarf galaxies (as suggested by the observations), it is difficult to reconcile the observed high total mass-to-light ratios in dwarf spheroidal galaxies (dSphs) with those of their simulated halos under the CDM paradigm. This discrepancy might be solved with a different way of galaxy formation.

An issue that remains unanswered is whether the same feedback recipes used in dwarf galaxies work as well in LSBs. As pointed out in Kuzio de Naray & Spekkens (2011) this seem unlikely, it is necessary to show that there is an accord between the content of gas in LSBs (usually low) and the large amount of it needed in CDM simulations (Brook et al. 2012; Stinson et al. 2011; Guo et al. 2010; More et al. 2011; Kuzio de Naray & Kaufmann 2011). We know LSBs are a large portion of the total galaxies that are observed (e.g., McGaugh et al. 1995), therefore, as far as there is not yet an agreement with LSBs and CDM simulations it worths exploring alternative models that provide a solution to the above disagreements.

There are several models in the literature that are addressing these and some other problems (Avila-Reese et al. 2001; Cembranos et al. 2005; Strigari et al. 2007; Spergel & Steinhardt 2000; Magaña et al. 2012a). Models that slightly modify CDM, like the warm dark matter (WDM) and self-interacting dark matter (SIDM) models, haven't been able to solve these discrepancies yet (Navarro et al. 2010; Kuzio de Naray & Spekkens 2011; Zavala et al. 2009; Davé et al. 2001; Yoshida et al. 2000). There are models that modify gravity like  $f(R)$  theories (De Felice & Tsujikawa 2010) and MOND (Milgrom 2010; Sanders 2009), but they are currently more at the effective-theory level

rather than at a fundamental one. Nevertheless, there are some rotation curves fits of LSBs galaxies in MOND models whose fits are almost perfect to the observed data (Sanders 2009).

One model that has received much attention is the scalar field dark matter (SFDM) model. It is our aim to show that in this model there is an scenario of galaxy formation (described in section 2) different from the standard model used in CDM simulations and that naturally produces core density profiles, reproduces rotation curves of large and small galaxies on equal footing as MOND and empirical dark matter models do, but that doesn't require large amounts of feedback. In previous works it has been verified that the SFDM model reproduces cosmological observations as well as CDM (Rodríguez-Montoya et al. 2010; Suárez & Matos 2011; Robles & Matos 2012; Magaña et al. 2012a; Böhrer & Harko 2007; Harko 2011).

This article is organized as follows, in section 2 we describe the SFDM model to be analysed in this paper, in section 3 we give our results and section 4 is devoted to discussion and conclusions.

## 2. SFDM model

### 2.1. Previous work and unsolved issues

The idea was first considered by Sin (1994) and independently introduced by Guzmán & Matos (2000). In the SFDM model the main hypothesis is that the dark matter is an auto-interacting real scalar field that condensates forming Bose-Einstein Condensate (BEC) "drops" (Magaña et al. 2012a). Then we interpret these BEC drops as the halos of galaxies, such that its wave properties and the Heisenberg uncertainty principle stop the DM phase-space density from growing indefinitely, and thus, it avoids cuspy halos and reduces the number of small satellites (Hu, Barkana & Gruzinov 2000).

In the SFDM model, the scenario of galaxy formation proposes that galactic halos form by condensation of a scalar field (SF) with an ultra-light mass of the order of  $m \sim 10^{-22}\text{eV}$  (units where the speed of light  $c=1$ ). From this mass it follows that the critical temperature of condensation  $T_{\text{crit}} \sim m^{-5/3} \sim \text{TeV}$  is very high, thus, they form BEC drops very early in the universe. It has been proposed that these drops are the halos of galax-

ies (Matos & Ureña 2001), *i.e.*, that halos are gigantic clumps of SF. The DM halos can be described in the non-relativistic regime, where DM halos can be seen as a Newtonian gas. When the SF has self-interaction, we need to add a quartic term to the SF potential and in the Newtonian limit the equation of state of the SF is that of a polytrope of index 1 (Suárez & Matos 2011; Harko 2011). On the other hand, big structures form like in the CDM model, by hierarchy (Matos & Ureña 2001; Suárez & Matos 2011), thus, all predictions of the CDM model at big scales are reproduced by SFDM.

Different issues of DM halos and the cosmological evolution of the SFDM model have been investigated in Colpi et al. (1986); Gleiser (1988); Matos & Ureña (2001); Chavanis (2011). Although the model is notably successful, there are at least two reasons to complement the model in addition to finding an explanation to the two discrepancies discussed in the introduction.

One of them is found when we consider the fully condensed system at temperature  $T=0$ , the fits to rotation curves (RCs) of LSBs (Robles & Matos 2012; Böhmer & Harko 2007) show deviations from the observed data at large radii because DM halos are modeled only by considering the ground state (complete condensation), whose DM density and velocity profile are given by (Böhmer & Harko 2007)

$$\rho^0(r) = \rho_0^0 \frac{\sin(\pi r/\hat{R})}{\pi r/\hat{R}}, \quad (1a)$$

$$V_0^2(r) = \frac{4\pi G \rho_0^0}{K^2} \left( \frac{\sin(Kr)}{Kr} - \cos(Kr) \right) \quad (1b)$$

where  $K = \pi/\hat{R}$ ,  $\rho_0^0 = \rho^0(0)$  is the central density, and the halo radius determined by  $\rho(\hat{R}) = 0$  is

$$\hat{R} = \pi \sqrt{\frac{\hbar^2 b}{Gm^3}}, \quad (2)$$

with  $\hbar$  is Planck's constant divided by  $2\pi$ ,  $m$  the mass of the DM particle,  $G$  the gravitational constant, and  $b$  the scattering length. The density profile depends on two fitting parameters, the central density and a length scale  $\hat{R}$ . However,  $\hat{R}$  depends only on fixed parameters, the interaction parameter  $\lambda$  and the mass of the SF particle, which implies that it should not vary from galaxy to galaxy. However, when fitting rotation curves of

galaxies, as  $\hat{R}$  is a fitting parameter it gets different values for each galaxy (Robles & Matos 2012; Böhmer & Harko 2007), this is something contradictory and represents a problem for the simplest SFDM model.

A second problem lies in the fast decrease of the velocity profile (equation (1b)) after its maximum value, such decrease causes a disagreement between the fits and the observed data in large galaxies because the data usually remain “flat” until the outermost regions (Swaters et al. 2000). In addition to this, and for large galaxies, when we aim for the best fit to the velocity maximum, we obtain a worse fit in the outer regions, *i.e.* the better the fit to the velocity maximum in the RC the worse the fit becomes in the outer regions and viceversa.

One approach to solve the problems was considered by Matos & Ureña (2007), and later by Harko & Madarassy (2011). It consisted in including finite temperature of dark matter in the DM halos. Harko & Madarassy (2011) show that by including a small correction to the pure condensed state, albeit in a different way from the one in this paper, it is possible to solve the first and partially solve the second discrepancy. The inclusion of temperature  $T$ , does mainly two things: 1) it makes the halo radius temperature-dependent, thus it's not fixed for all galaxies anymore and 2) it lifts the RC fit in the outer region and keeps it flat until the last value. However, effect 2) is negligible when the halo temperature is  $T < 0.5 T_{\text{BEC}}$ , where  $T_{\text{BEC}}$  is the critical temperature of Bose Einstein condensation, if  $T_{\text{BEC}} \sim \text{TeV}$ , we would expect present halos to be well approximated by equation (1b) and hence, we will be unable to simultaneously obtained a good fit to the RC maximum and the RC outer regions. Though this last problem is not readily visible in galaxies with small radius (outer radius of  $\leq 10$  kpc), it is notable in large galaxies, therefore problem 2) is just partially solved.

Thus, an alternative approach to solve these two SFDM discrepancies considers non-condensed SF configurations at  $T=0$ , *i.e.* SF configurations in excited states (Balakrishna et al. 1998; Ureña & Bernal 2010; Bernal et al. 2010). These configurations fit RCs up to the last data point and can even reproduce the wiggles seen at large radii in high-resolution observations (Sin 1994;

Colpi et al. 1986). The problem found in this type of solution was that the configurations required for the fits (4-5 exited states) were unstable and decayed to the ground state in a short time (Siddhartha & Ureña 2003). Therefore, we will expect to see today that most DM halos are in their ground state, which means that the disagreement at large radii would remain.

## 2.2. Finite Temperature SF scenario

Motivated to solve all these issues we consider the following scenario which includes temperature of the DM and the exited states of the SF.

The idea is that the dark matter is a scalar field, we consider a real SF  $\Phi$ , with a repulsive interaction embedded in a thermal bath of temperature  $T$ , we also consider the finite temperature corrections up to one-loop in the perturbations. This is described by the potential (Kolb & Turner 1987; Dalfovo et al. 1999)

$$V(\Phi) = -\frac{1}{2} \frac{\hat{m}^2 c^2}{\hbar^2} \Phi^2 + \frac{\hat{\lambda}}{4} \Phi^4 + \frac{\hat{\lambda}}{8} k_B^2 T^2 \Phi^2 - \frac{\pi^2 k_B^4 T^4}{90 \hbar^2 c^2}. \quad (3)$$

for the case when  $k_B T \gg \hat{m} c^2$ . Here  $k_B$  is Boltzmann's constant,  $\hat{\lambda} = \lambda/(\hbar^2 c^2)$  is the parameter describing the interaction,  $\hat{\mu}^2 := \hat{m}^2 c^2/\hbar^2$  is a parameter, and  $T$  is the temperature of the thermal bath. The first term in  $V(\Phi)$  relates to the mass term, the second to the repulsive self-interaction, the third to the interaction of the field with the thermal bath, and the last to thermal bath only.

At some high enough temperature in the early universe, when the SF reaches the minimum of the potential ( $\Phi \approx 0$ ) it behaves as dust, reproducing all the features of the CDM model at cosmological scales. In this period the SF interacts with the rest of the matter, eventually, when the temperature is sufficiently small the SF decouples from the interaction with the rest of the matter and follows its own thermodynamic history, cooling down with the universe expansion. After this moment and for sufficiently low  $T$ , the term proportional to  $T^4$  is not longer important and can be dropped out. Moreover, as the temperature continues decreasing, the initial minimum of the potential in  $\Phi=0$  eventually becomes a local maximum, after this happens the initial  $Z_2$  symmetry of the potential  $V(\Phi)$  is broken. The latter happens at a

critical temperature  $T_C$  given by

$$k_B T_C = \frac{2\hat{m}c^2}{\sqrt{\lambda}}. \quad (4)$$

The critical temperature  $T_C$  determines the moment in which the DM fluctuations can start growing, they do it from the moment when  $T < T_C$  until they reach a stable equilibrium point, for example in  $\Phi_{\min}^2 = k_B^2 (T_C^2 - T^2)/4$  (see section 2.3).

## 2.3. Evolution equations

The perturbed system of a scalar field with a quartic repulsive interaction but with temperature zero has been studied by many authors (Colpi et al. 1986; Ureña & Bernal 2010). Following the same procedure we study the evolution of the SF in a FRW universe. We write the metric tensor as  $\mathbf{g} = \mathbf{g}^0 + \delta\mathbf{g}$ , where  $\mathbf{g}^0$  is the unperturbed FRW background metric, and  $\delta\mathbf{g}$  the perturbation. The perturbed line element in conformal time  $\eta$ , is (we take  $c=1$  in this subsection)

$$ds^2 = a(\eta)^2 [-(1+2\psi)d\eta^2 + 2B_{,i}d\eta dx^i + a(\eta)^2 [(1-2\phi)\delta_{ij} + 2E_{,ij}]dx^i dx^j], \quad (5)$$

with  $a$  the scale factor,  $\psi$  the lapse function,  $\phi$  gravitational potential,  $B$  the shift, and  $E$  the anisotropic potential. We separate the Energy-Momentum tensor and the field as  $\mathbf{T} = \mathbf{T}_0 + \delta\mathbf{T}$ , and  $\Phi(x^\mu) = \Phi_0(\eta) + \delta\Phi(x^\mu)$  respectively. As we are studying the linear regime  $\delta\Phi(x^\mu) \ll \Phi_0(\eta)$ , we can approximate  $V(\Phi) \approx V(\Phi_0)$ . We work in the Newtonian gauge where the metric tensor  $\mathbf{g}$  becomes diagonal and as a result, in the trace of the Einstein's equations the scalar potentials  $\psi$  and  $\phi$  are identical, therefore,  $\psi$  relates to the gravitational potential.

Changing to the cosmological time  $t$  using the relation  $(d/d\eta) = a(d/dt)$ , the perturbed Einstein's equations  $\delta G_j^i = 8\pi G \delta T_j^i$  to first order for an scalar field in the Newtonian gauge ( $E=0=B$ ) are

$$-8\pi G \delta \rho_\Phi = 6H(\dot{\phi} + H\phi) - \frac{2}{a^2} \nabla^2 \phi, \quad (6a)$$

$$8\pi G \dot{\Phi}_0 \delta \Phi_{,i} = 2(\dot{\phi} + H\phi)_{,i}, \quad (6b)$$

$$8\pi G \delta p_\Phi = 2[\ddot{\phi} + 3H\dot{\phi} + (2\dot{H} + H^2)\phi]6c$$

with  $\dot{\phantom{x}} = \partial/\partial t$  and  $H = (\ln a)$ . In this gauge  $\mathbf{g}$  is diagonal thus  $\phi = \psi$ . The perturbed density  $\delta\rho_\Phi$  and the perturbed pressure  $\delta p_\Phi$  are defined in

terms of the perturbed energy momentum tensor as

$$\begin{aligned}\delta T_0^0 &= -\delta\rho_\Phi = -(\dot{\Phi}_0\delta\dot{\Phi} - \dot{\Phi}_0^2\psi + V_{,\Phi_0}\delta\Phi), \\ \delta T_i^0 &= -\frac{1}{a}(\dot{\Phi}_0\delta\Phi_{,i}), \\ \delta T_j^i &= \delta p_\Phi = (\dot{\Phi}_0\delta\dot{\Phi} - \dot{\Phi}_0^2\psi - V_{,\Phi_0}\delta\Phi)\delta_j^i.\end{aligned}\quad (7)$$

Systems (6) and (7) describe the evolution of the scalar perturbations. To study the evolution of the SF perturbations we use the perturbed Klein-Gordon equation

$$\begin{aligned}\ddot{\delta\Phi} + 3H\delta\dot{\Phi} - \frac{1}{a^2}\nabla^2\delta\Phi + V_{,\Phi_0\Phi_0}\delta\Phi + \\ + 2V_{,\Phi_0}\dot{\phi} - 4\dot{\Phi}_0\dot{\phi} = 0.\end{aligned}\quad (8)$$

Equation (8) can be rewritten as:

$$\square\delta\Phi + \left.\frac{d^2V}{d\Phi^2}\right|_{\Phi_0}\delta\Phi + 2\left.\frac{dV}{d\Phi}\right|_{\Phi_0}\dot{\phi} - 4\dot{\Phi}_0\dot{\phi} = 0, \quad (9)$$

where the D'Alembertian operator is defined as

$$\square := \frac{\partial^2}{\partial t^2} + 3H\frac{\partial}{\partial t} - \frac{1}{a^2}\nabla^2. \quad (10)$$

Essentially equation (8) represents a harmonic oscillator with a damping  $3H\delta\dot{\Phi}$  and an extra force  $-2\phi V_{,\Phi_0}$ . Equation (8) has oscillating solutions if the term  $(V_{,\Phi\Phi} - \frac{1}{a^2}\nabla^2)\delta\Phi$  is positive. This equation contains growing solutions if this term is negative, that is, if  $V_{,\Phi\Phi}$  is negative enough. From here we see an important feature. These perturbations grow only if  $V$  has a maximum, even if this is a local one. Here the potential is unstable and during the time when the scalar field remains in the maximum, the scalar field fluctuations grow until they reach a stable point. This implies that the galactic halos could have formed within this period and with similar features. Finally for the background field equation we have that  $\dot{\phi}\approx 0$ , therefore its equation reads

$$\ddot{\Phi}_0 + 3H\dot{\Phi}_0 + V_{,\Phi}(\Phi_0) = 0. \quad (11)$$

We have that  $\Phi_0$  depends only on time, we now suppose that the temperature is sufficiently small so that the interaction between the SF and the rest of matter has decoupled, and we assume that the symmetry break (SB) took place in the radiation

dominated era in a flat universe, in this case the equation for the SF perturbations reads

$$\begin{aligned}\square\delta\Phi + \frac{\hat{\lambda}}{4}[k_B^2(T^2 - T_C^2) + 12\Phi_0^2]\delta\Phi - 4\dot{\Phi}_0\dot{\phi} \\ + \frac{\hat{\lambda}}{2}[k_B^2(T^2 - T_C^2) + 4\Phi_0^2]\Phi_0\phi = 0\end{aligned}\quad (12)$$

In Figure 1 we show the behavior of the potential for different temperatures, we see that the SB takes place at  $T=T_C$ .

In Magaña et al. (2012b) they solve numerically the evolution of the fields  $\Phi_0$  and  $\delta\Phi$  that satisfy (6), (7), (11) and (12). They show that as the temperature decreases and goes below  $T_C$ ,  $\Phi_0$  falls rapidly to a new minimum where it will remain oscillating. In a similar way, the SF fluctuation grows very quickly only when  $\Phi_0$  approaches the minimum. Taking  $\Phi\approx 0$  when  $T>T_C$ , the behavior of the field  $\Phi$  just after the SB is what we had expected, i.e, it changed from being a local minimum to an unstable local maximum of the potential rolling down to the minimum  $\Phi_{\min}$ . It is in this period when the SF fluctuation can grow. Hence, it is only before the SB when the SF remains homogeneous.

From here we see that in the SFDM model, the primordial DM halos form almost at the same time due to the phase transition produced by the SB. In the non-linear regime these halos can merge with other halos forming larger structures just like in the CDM model. However, the main difference lies in the initial formation of the DM halos, they are formed very rapidly and almost at the same time, from here we expect that they possess similar features. This difference between the SFDM and CDM models can be tested by observing well formed high-redshift galaxies and also by comparing characteristic parameters of several DM dominated systems, for instance, by observing that indeed, dwarf or LSB galaxies possess cores even at high-redshift, especially since CDM simulations of dwarf galaxies by Governato et al. (2012) suggest that their DM density profiles were initially cuspy but later on turn into core profiles due to feedback processes.

## 2.4. Newtonian limit

In this work we are interested in the galaxy after its formation. Thus, we constrain ourselves

to solve the static limit of equation (12) when  $\Phi$  is near the minimum of the potential and after the SB, where we expect it to be stable. We also expect the gravitational potential to be locally very homogeneous in the beginning of its collapse, therefore the gravitational potential  $\dot{\phi} \approx 0$ . The stability of these halos will be shown elsewhere. For clarity, from here on we stop using units in which  $c=1$ . We find an exact spherically symmetric static solution for the SF when it is near the minimum of the potential ( $V'(\Phi)|_{\Phi_0} \approx 0$ ), i.e., when  $\Phi_0^2 = \Phi_{\min}^2 = k_B^2 (T_C^2 - T^2)/4$  and  $T < T_C$ . For the static case  $H = 0$ ,  $\dot{\Phi}_0 \approx 0$  and equation (12) reads

$$\delta\ddot{\Phi} - \nabla^2 \delta\Phi + \frac{\lambda k_B^2}{2\hbar^2} (T_C^2 - T^2) \delta\Phi = 0. \quad (13)$$

Equation (13) describes the evolution of the fluctuations of the SF after the SB. Moreover, this equation is linear. In the SFDM model these fluctuations describe the DM halos, therefore, a solution of this system is equivalent to obtaining the temperature corrected density profile of early DM halos.

We find that the ansatz

$$\delta\Phi = \delta\Phi_0 \frac{\sin(kr)}{kr} \cos(\omega t) \quad (14)$$

is an exact solution to equation (13) provided

$$\omega^2 = k^2 c^2 + \frac{\lambda k_B^2}{2\hbar^2} (T_C^2 - T^2). \quad (15)$$

From equation (15) we notice that now  $k$  depends on the temperature  $T$ . If we use the Madelung representation (Barcelo et al. 2005) we find an easier interpretation of the solution (14). We write

$$\delta\Phi = \frac{2\sqrt{n}}{\sqrt{2}\kappa} \cos(S - \mu ct), \quad (16)$$

$$\phi = 2\sqrt{q} \cos(Q - \mu ct) \quad (17)$$

where the phases  $S(x, t)$ ,  $Q(x, t)$ , and the functions  $n(x, t)$  and  $q(x, t)$  are taken as real functions. The reason of introducing  $\kappa$  is that it gives us the necessary units so that we can interpret  $n(x, t)$  as the number density of DM particles, as  $\Phi$  has energy units. With this in mind, we can define an effective mass density of the SF fluctuation by  $\rho = mn$ .

Combining equations (14) and (16) and using our interpretation of  $n$  we obtain a finite temperature density profile

$$\rho(r) = \rho_0 \frac{\sin^2(kr)}{(kr)^2}, \quad (18)$$

provided

$$k_B^2 T^2 = k_B^2 T_C^2 - 4\Phi_0^2, \quad (19)$$

$$S = \omega t + \frac{mc^2}{\hbar} t. \quad (20)$$

$$\Phi_0^2 = \Phi_{\min}^2 \quad (21)$$

Here  $k=k(T)$  and  $\rho_0=\rho_0(T)$  are fitting parameters while  $\lambda$ ,  $T_C$ ,  $\kappa$  are free parameters to be constrained by observations. For galaxies the Newtonian approximation gives a good description, therefore, from equation (18) we obtain the mass and rotation curve velocity profiles given by

$$M(r) = \frac{4\pi G \rho_0}{k^2} \frac{r}{2} \left( 1 - \frac{\sin(2kr)}{2kr} \right), \quad (22a)$$

$$V(r)^2 = \frac{4\pi G \rho_0}{2k^2} \left( 1 - \frac{\sin(2kr)}{2kr} \right). \quad (22b)$$

respectively. Lately, the Einasto DM profile seems to give a better description of DM halos in CDM simulations (Navarro et al. 2010; Merrit et al. 2006; Graham et al. 2006), we include the Einasto RC profile for a later comparison with (22b),

$$V_E^2 = 4\pi G \rho_{-2} \frac{r_{-2}^3}{r} \left[ \frac{e^{2/\alpha}}{\alpha} \left( \frac{\alpha}{2} \right)^{(3/\alpha)} \gamma\left(\frac{3}{\alpha}, x'\right) \right], \quad (23)$$

with  $\gamma$  the incomplete gamma function given by

$$\gamma\left(\frac{3}{\alpha}, x'\right) = \int_0^{x'} e^{-t} t^{(3/\alpha)-1} dt$$

and  $x' := \frac{2}{\alpha} \left( \frac{r}{r_{-2}} \right)^\alpha$ .

We now define the radius  $R$  of the SFDM distribution by the condition  $\rho(R) = 0$ . This fixes the relation

$$k_j R = j\pi, \quad j = 1, 2, 3, \dots \quad (24)$$

where  $j$  is the number of the exited state required to fit a galaxy RC up to the last measured point. From equations (13) and (24) we find that the halo

allows exited states and then, the total density is the sum of densities in the different states.

We notice that the profile in equation (18) presents “wiggles,” characteristic of configurations in exited states (Sin 1994). Also, we define the distance where the first peak (maximum) in the RC is reached as  $r_{\max}^1$ , this determines the first local maximum of the RC velocity, which can be obtained from equation (25)

$$\frac{\cos(2\pi jy)}{2(\pi j)^2 y} \left[ \frac{\tan(2\pi jy)}{2\pi jy} - 1 \right] = 0, \quad (25)$$

where we used equation (24) and  $y := (r_{\max}^1/R)$ .

### 3. Discussion

We have seen that within our scenario of dark matter and galaxy formation the DM halos are naturally cored, i.e., their central density profiles are finite and do not diverge, on the contrary, they behave as  $\rho \sim r^0$  for small  $r$ , it is important to note that the core is obtained from the model and not assumed, thus, this is an alternative way to solve the cusp/core discrepancy without adding baryons (Kuzio de Naray & Kaufmann 2011).

In the SFDM model the DM halos (density fluctuations) form after the SB and grow only after the field rolls to the minimum of the potential, same which varies with the temperature  $T$ . Therefore, the initial size of the fluctuation depends on the temperature at which it formed. From equation (15) we see that the size of the DM configuration, specified by  $R$ , is now temperature-dependent, therefore, as in Harko & Madarassy (2011), we also solve the problem of a unique scale length for all halos, but now by using the SB mechanism. Therefore, halos which formed at different temperatures may have different sizes (values of  $R$ ).

In Figure 2 we show the RC fits of three LSB galaxies using the minimum disk hypothesis (neglecting the baryonic component) taken from a high-precision subsample of McGaugh (2005), we compare equation (22b) (solid line) and equation (23) (dashed line) and notice that these galaxies present two features, long flat tails in the outer region and wiggles. The wiggles (small oscillations) are perfectly reproduced by the SFDM model by using combinations of exited states, the letter  $j$  that appears in the panels of Figure 2 specifies

the required combination of states. It is important to highlight the SFDM fit of NGC 1560, we note it has the same great level of accuracy displayed in MOND models (Gentile et al. 2010; Sanders 2009). This combination of states in our RC fits suggests that there is not a universal DM profile, but instead, that the subsequent evolution determines the final profile. The flat outermost region is a consequence of considering exited states, same behavior that was present in previous works (Sin 1994; Bernal et al. 2010) which used  $T=0$ . However, the main difference now is that by considering  $T \neq 0$  we can accommodate exited states in halos and expect them to be stable due to the DM thermal and repulsive self interactions. Moreover, by considering for the first time both finite DM temperature corrections and exited states, we obtained an excellent agreement with the observed data (see Figure 2), suggesting that large quantities of baryons are not essential to fit RCs in our model. This precludes the necessity of including large amounts of gas, stars, and feedback processes to flatten the inner regions of RCs. We expect that adding only the observed amount of baryons will be enough to reach perfect agreement with RC observations and the correct luminosity. This will be seen in future works.

Regarding the second problem about fitting the maximum of the RC and the outer regions at the same time, we notice from Figure 2 that we do not have such problem anymore, in contrast to previous works (Harko 2011; Harko & Madarassy 2011; Robles & Matos 2012), the difference is mainly due to the combination of states in halos. We can estimate a lower bound of  $j$ , the minimum exited state necessary to agree with the data up to the last measured point, with the following rule of thumb: we find the value of  $y$  by identifying from the RC the last measured point as  $R$  and the first maximum (first visible peak) as  $r_{\max}^1$ , we look for the closest value of  $j$  associated with this  $y$  in Figure 3 (the values of Figure 3 are determined by equation (25)), this provides us with the dominant state in the center of the galaxy and at the same time with the minimum state required to fit current observations. It is a lower bound because upcoming observations might go beyond  $R$ , in that case  $R$  will increase and  $y$  will decrease, implying larger values of  $j$ .

As some final remarks we see from Figure 2

that Einasto fits are in general agreement in the outer regions, but the wiggles cannot be reproduced with DM only. In fact, if we want to reproduce the oscillations seen in high-resolution RCs with a non-oscillatory DM profile (NFW, Einasto's, Burkert's etc.), we must include the gas and stars dynamics in the simulations, it would be interesting to show the stability of the oscillations after including baryons, as this might be a challenging task in LSBs galaxies due to their low gas content.

In addition to the fact that the approximation to the data by the Einasto profile is good, except for the wiggles and possibly the central region, we notice that the parameter  $\alpha$  changes for each galaxy. As noted in previous works (Merri et al. 2006; Navarro et al. 2010; Jin & Suto 2000; Gentile et al. 2007), the change in  $\alpha$  implies that halos do not possess a universal profile, i.e., if we take Einasto profile to be the best representation of the simulated DM halos in a CDM environment, then we should expect to see a non-universality in the halos of galaxies, this is just the same result we have obtained directly from the SFDM model but without assuming a priori a DM density profile.

#### 4. Conclusions

In this paper we give an extension to the SFDM model that includes the DM temperature corrections to the first loop in perturbations. We propose a  $Z_2$  spontaneous symmetry break of a real scalar field as a new mechanism in which the early DM halos form. When the real scalar field rolls down to the minimum of the potential, the perturbations of the field can form and grow. We give an exact analytic solution for an static SF configuration, which in the SFDM model represents a DM halo. This solution naturally presents a flat central density profile, it can accommodate more than just the ground state as now the temperature  $T \neq 0$ , and solves previous discrepancies in rotation curve fits at  $T=0$ , for instance, having a constant halo radius for all galaxies and, in the case of large galaxies, the incapability to fit at the same time the inner and outermost regions of RCs.

Additionally to solving these two disagreements we showed that there is no need to include high amounts of feedback to fit and reproduced the in-

ner core and “wiggles” found in high-resolution RCs. Also, the model can be tested with high redshift observations, the SF model predicts initial core profiles as opposed to the initially cuspy ones found in CDM simulation which are expected to flatten due to redistribution of DM by astrophysical processes. Finally, both the Einasto and SFDM RC fits suggest the non-universality of the DM halos, though the latter claim is still not final and further work has to be done in such direction. We strongly believe that exploring further the SFDM looks promising to unravel the mystery of dark matter.

This work was supported in part by DGAPA-UNAM grant IN115311 and by CONACyT Mexico grant 49865-E.

#### REFERENCES

- Avila-Reese, V., Colín, P., Valenzuela, O., DOnghia, E., & Firmani, C. 2001, *ApJ*, 559, 516
- Balakrishna, J., Seidel, E., Suen, W.-M. 1998, *Phys. Rev. D*, 58, 104004
- Barcelo, C., Liberati, S., & Visser, M. 2005, *Living Rev. Rel.*, 8, 12
- Bernal, A., Barranco, J., Alic, D., & Palenzuela, C. 2010, in *AIP Conf. Proc.*, 1083, 20-27
- Böhmer, C.G., & Harko, T. 2007, *JCAP*06, 025
- Brook, C.B., Stinson, G., Gibson, B.K., Wadley, J. & Quinn, T. 2012, *MNRAS*, preprint (10.1111/j.1365-2966.2012.21306.x)
- Burkert, A. 1995, *ApJ*, 447, L25
- Cembranos, J. A. R., Feng, J. L., Rajaraman, A., & Takayama, F. 2005, *Physical Review Letters*, 95, 181301
- Chavanis, P.H. 2011, *Phys. Rev. D*, 84, 043531
- Colpi, M., Shapiro, S.L., & Wasserman, I. 1986, *Phys. Rev. Lett.*, 57, 2485
- Dalfovo, F., Giorgino, S., Pitaevskii, L. P., Stringari, S. 1999, *Rev. Mod. Phys.*, 71, 463
- Davé, R., Spergel, D.N., Steinhardt, P.J., & Wandelt, B.D. 2001, *ApJ*, 547, 574



- de Blok, W.J.G. et al., 2001, *ApJ*, 552, L23
- de Blok, W.J.G. 2010, *Adv. Astron.*, 2010, Article ID 789293, 14 pages.
- De Felice, A., & Tsujikawa, S. 2010, *Living Rev.Rel.* 13, 3, <http://www.livingreviews.org/lrr-2010-3>
- Gentile, G., Tonini, C., & Salucci, P. 2007, *A&A*, 467, 925
- Gentile, G., Baes, M., Famaey, B., Van Acoleyen, K. 2010, *MNRAS*, in press (arXiv:1004.3421)
- Gleiser, M. 1988, *Phys. Rev. D*, 38, 2376
- Graham, A.W., Merrit, D., Moore, B., Diemand, J., & Terzić, B. 2006, *ApJ*, 132, 2701
- Governato, F. et al., 2010, *Nature*, 463, 203
- Governato, F. et al., 2012, *MNRAS*, in press (arXiv:1202.0554v2)
- Guo, Q., White, S., Li, C., & Boylan-Kolchin, M. 2010, *MNRAS*, 404, 1111
- Guzmán, F.S., & Matos, T. 2000, *Class. Quant. Grav.*, 17, L9
- Harko T., 2011, *MNRAS*, 413, 3095
- Harko, T., & Madarassy, E.J.M. 2011, *JCAP*01, 020
- Hu, W., Barkana, R., & Gruzinov, A. 2000, *Phys. Rev. Lett.*, 85, 1158
- Jin, Y.P., & Suto, Y. 2000, *ApJ*, 529, L69
- Kuzio de Naray, R. et al., 2010, *ApJ*, 710, L161
- Kuzio de Naray, R. & Spekkens, K. 2011, *ApJ*, 741, L29
- Kuzio de Naray, R., Kaufmann, T. 2011, *MNRAS*, 414, 3617
- Kolb, E., & Turner, M. 1987, *The Early Universe*, Addison-Wesley
- Maccio, A.V. et al., 2011, *ApJL*, in press (arXiv:1111.5620v1)
- Magaña, J., Matos, T., Robles, V.H., Suárez, A. 2012a, *Proceedings of the XIII Mexican Workshop on Particles and Fields*, in press (arXiv:1201.6107v1)
- Magaña, J., Matos, T., Suárez, A., Sánchez-Salcedo, F.J. 2012b, *JCAP*, submitted (arXiv:1204.5255v1)
- Matos, T., & Ureña-López, L.A. 2007, *Gen Relativ Gravit*, 39, 1279
- Matos, T., Ureña-López, L.A. 2001, *Phys Rev. D*, 63, 063506
- McGaugh, S.S., Bothun, G.D., & Schombert, J.M. 1995, *AJ*, 110, 573
- McGaugh, S.S. 2005, *ApJ*, 632, 859
- Merrit, D., Graham, A.W., Moore, B., Diemand, J., & Terzić, B. 2006, *ApJ*, 132, 2685
- Milgrom, M. 2010, *AIP Conf.Proc.*, 1241, 139
- More, S., van den Bosch, F.C., Cacciato, M., Skibba, R., Mo, H.J., & Yang, X. 2011, *MNRAS*, 410, 210
- Navarro, J.F. et al., 2010, *MNRAS*, 402, 21
- Oh, S.H., de Blok, W.J.G., Brinks, E., Walter, F., & Kennicutt, R.C. Jr. 2011, *AJ*, 141, 193
- Robles, V. H., & Matos, T. 2012, *MNRAS*, 422, 282
- Rodríguez-Montoya, I., Magaña, J., Matos, T., Pérez, L.A. 2010, *ApJ*, 721, 1509
- Romano-Daz, E. et al., 2008, *ApJ*, 685, L105
- Sanders, R.H., 2009, *Adv. Astron.*, Article ID 752439
- Sawala, T., Scannapieco, C., & White, S. 2012, *MNRAS*, 420, 1714
- Siddhartha, F.G., & Ureña-López, L.A. 2003, *Phys. Rev. D*, 68, 024023
- Sin, S.J. 1994, *Phys. Rev. D*, 50, 3650
- Spergel, D. N., & Steinhardt, P. J. 2000, *Physical Review Letters*, 84, 3760
- Stinson, G.S. et al., 2011, arXiv:1112.1698v1
- Strigari, L. E., Kaplinghat, M., & Bullock, J. S. 2007, *Phys. Rev. D*, 75, 061303
- Suárez, A., & Matos, T. 2011, *MNRAS*, 416, 87

- Swaters, R.A., Madore, B.F., & Trehella, M. 2000, ApJ, 531, L107
- Ureña-López, L.A., & Bernal, A. 2010, Phys. Rev. D, 82, 123535
- van Eymeren, J., Trachternach, C., Koribalski, B.S., & Dettmar, R.J. 2009, A&A, 505, 1
- Villaescusa-Navarro, F., Dalal, N. 2011, JCAP03(2011)024
- Yoshida, N., Springel, V., White, S.D.M., & Tormen, G. 2000, ApJ, 544, L87
- Zavala, J. et al., 2009, ApJ, 700, 1779

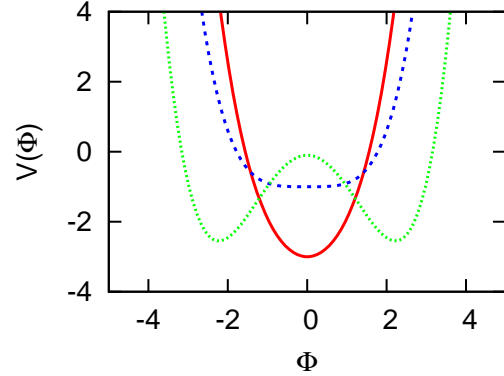


Fig. 1.— We plot the qualitative behavior of  $V(\Phi)$  vs  $\Phi$  for three different values of  $T$ . The solid line (red in the online version) is when  $T > T_C$ , here the system oscillates around the minimum and possesses a  $Z_2$  symmetry, the dashed line (blue in the online version) is when the SB takes place, this happens when  $T = T_C$ , and the dotted line (colored green in the online version) is for  $T < T_C$ , in this period  $\Phi$  can roll down to a new minimum and there is no longer  $Z_2$  symmetry.

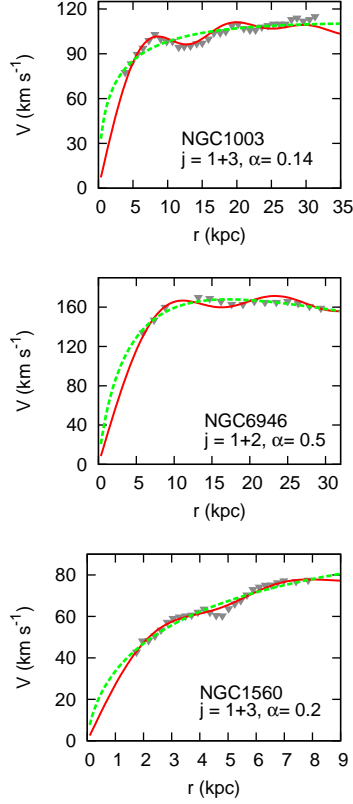


Fig. 2.— Rotation curve fits to three LSB galaxies. *top panel*: NGC 1003, *middle panel*: NGC 6946, *bottom panel*: NGC 1560. Solid lines (red in the online version) are the fits using the SFDM model, dashed line (green in the online version) represents Einasto's fits, and triangles are the observational data. In NGC 1560 we see that the dip at  $r \approx 5$  kpc is reproduced more accurately in the SFDM profile. Einasto fits show different values of  $\alpha$  in each galaxy, suggesting a non-universality in the DM halos, the same is concluded in the SFDM model.

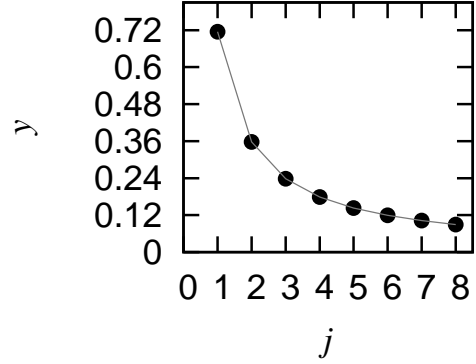


Fig. 3.— We plot the relation between  $y$  and  $j$  obtained by solving equation (25). Notice that for halos with large excited states (large  $j$ ), the first maximum is attained at a smaller  $y$ .